

Central European Journal of Energetic Materials

ISSN 1733-7178; e-ISSN 2353-1843

Copyright © 2025 Łukasiewicz Research Network – Institute of Industrial Organic Chemistry, Poland

Cent. Eur. J. Energ. Mater. 2025, 22(3): 344-361; DOI 10.22211/cejem/211476

Supporting Information is available in PDF-format, in colour, at: https://ipo.lukasiewicz.gov.pl/wydawnictwa/cejem-woluminy/vol-22-nr-3/



Article is available under the Creative Commons Attribution-Noncommercial-NoDerivs BY NC ND 3.0 license CC BY-NC-ND 3.0.

Research paper

Influence of Nitramine Explosives on the High-Pressure **Combustion Behaviour and Mechanical Properties of Mixed-Ester Nitramine Propellants**

Jun Dong^{1,2,*)}, Jinyu Peng²⁾, Chunzhi Li²⁾, Jiangyang Ou²⁾, Jinrui Liu²⁾

- 1) School of Chemistry and Chemical Engineering, Nanjing University of Science and Technology, Nanjing, Jiangsu, 210094, China
- ²⁾ Luzhou North Chemical Industries Co., Ltd, Luzhou 646003. China
- * E-mail: 19038142369@163.com

Abstract: To investigate the effect of high-energy nitramine explosives on the performance of mixed ester-nitramine propellants, a closed bomb apparatus and mechanical property testing instruments were used. The combustion and mechanical properties of mixed ester-nitramine propellants containing nitramine explosives and different particle sizes of RDX, as well as three different highenergy formulations incorporating RDX (propellants ZTH-1 and ZTH-2), HMX (propellant ZTA), and CL-20 (propellant ZTC), were evaluated. The results indicate that the burning rate (U) of mixed ester-nitramine propellants varies with the RDX particle size, with larger RDX particles leading to a higher U. The U values of the three different types of nitramine propellant samples follows the order: U(ZTC) > U(ZTH-2) > U(ZTH-1) > U(ZTA). For the three different types of nitramine propellant samples, the ZTH-2 propellant exhibited the lowest pressure exponent, while the ZTC propellant had the highest pressure exponent. The impact strength followed the order: $\alpha_{\rm r}({\rm ZTH-2}) > \alpha_{\rm r}({\rm ZTA}) > \alpha_{\rm r}({\rm ZTH-1}) > \alpha_{\rm r}({\rm ZTC})$. The ranking of the low-temperature drop-weight impact strengths at -40 °C was as follows: [ZTA] > [ZTH-2] > [ZTH-1] > [ZTC].

Keywords: mixed ester-nitramine propellant, ammonium nitrate, closed bomb, combustion performance, burning rate pressure exponent, mechanical properties

1 Introduction

A propellant serves as the core energy source for barrel firearms, directly determining the muzzle velocity, power, and destructive effectiveness. With the increasing demand for higher muzzle velocity, enhanced power, and efficient lethality in modern warfare - particularly for tank guns and anti-tank firearms - research has focused on propellants with high-energy-density, high mechanical strength, and progressive combustion characteristics [1]. Traditional nitrocellulose-based propellants exhibit relatively balanced properties; however, their energy density and combustion performance are gradually becoming insufficient to meet the demands of modern weapon systems. Consequently, the development of novel high-energy-density propellants has become an urgent research priority [2, 3].

In recent years, significant progress has been made in applying novel high-energy-density compounds, e.g. 2,4,6,8,10,12-hexanitro-2,4,6,8,10,12hexaazaisowurtzitane (CL-20), 1,3,5-trinitro-1,3,5-triazinane (RDX), and (1,3,5,7-tetranitro-1,3,5,7-tetraazacyclooctane (HMX) in solid propellants and explosives [4]. These compounds possess high-energy-density and excellent detonation performance, which can substantially enhance the energy output of propellants. Researchers worldwide have extensively studied the application of these high-energy compounds in propellant formulations [5, 6]. Wu et al. [7] investigated the application of different crystalline forms of HMX in nitraminebased propellants and found that α -HMX exhibited superior ignition characteristics but lower gas-generation intensity, slower burning rates, and a higher burning rate pressure exponent. Zhang et al. [8] examined the effect of RDX content on the mechanical and combustion properties of nitramine propellants, revealing that while RDX significantly increases the energy output, its influence on the mechanical and combustion properties is complex. The test results showed that the impact strength of 30% RDX nitramine propellant was the largest, and that of 40% RDX nitramine propellant was the smallest. The highest crushing height was achieved with 20% RDX and the lowest with 40% RDX. Sinditskii et al. [9] studied the thermal decomposition characteristics of CL-20, providing a theoretical foundation for its application in propellants. Wei et al. [10] analyzed the compatibility, energy performance, and combustion behaviour of CL-20, 3,4-bis(3-nitrofurazan-4-yl)furoxan (DNTF), and ammonium dinitramide (ADN) in high-energy nitramine propellants (RGD7A), concluding that CL-20 and DNTF exhibit good compatibility with nitramine propellants while significantly enhancing their burning rate and burning rate pressure exponent.

Although the incorporation of high-energy-density compounds can markedly enhance the energy performance of propellants, it also introduces new challenges in combustion properties (which directly impact the interior ballistics of firearms) and mechanical properties (which determine the structural integrity and safety of propellants under high-temperature and high-pressure conditions) [11-13]. Furthermore, the influence of different particle sizes of high-energy-density compounds on propellant performance remains inadequately explored. To address these challenges, the present study employed a semi-solvent oil-pressing method to prepare three types of mixed ester-nitramine propellants and investigated the effects of two different RDX particle sizes on their combustion and mechanical properties. The findings of this study provide valuable insights for optimizing high-energy-density propellant formulations, enhancing their practical performance and safety, and supporting the advancement of modern weapon systems [14-16].

2 Raw Materials and Tested Propellants

The following raw materials were used:

- nitrocellulose, absorbent propellant, Yibin North Chuanan Chemical Industry Co., Ltd.,
- ethanol and acetone (analytically pure) Luzhou North Chemical Industry Co., Ltd.,
- plasticizer: nitroglycerin and triethylene glycol dinitrate, Luzhou North Chemical Industry Co., Ltd.,
- RDX type V (particle size: 20-45 μm), RDX ultrafine (particle size: 1-10 μm) and HMX (particle size: 20-45 μm) all of industrial grade, Gansu Yinguang Chemical Industry Group Co., Ltd.,
- CL-20, ε type, particle size: 20-45 μm, industrial grade, Liaoning Qingyang Special Chemical Co., Ltd.

The preparation of the propellants was carried out using the semi-solvent hydraulic pressing process (hydraulic press, XTM103C-3T, from Luzhou Northern Chemical Industry Co., Ltd., China). The molding pressure was 0~10 MPa, and the temperature was 25 °C. The main steps included absorption, tablet compression, plasticization, extrusion molding, as well as curing, cutting,

and drying. The resulting propellants had a 19-hole configuration; the aperture diameter was 0.35 mm, and the arc thickness was 1.8 mm. In the mixed ester nitramine propellant, the nitramine explosive component was added during the gelation process, where the mass ratio of ethanol to acetone solvent was 2:3. The formulation of the mixed ester nitramine propellants remained consistent in component content, with only the type and particle size of the nitramine propellants varying, as detailed in Table 1.

Mixed ester nitramine propellant	Nitramine explosive	Particle diameter [µm]	Nitramine explosive [%]	Nitrocel- lulose [%]	Plasti- cizer [%]	Other components [%]
ZTH-1	RDX	1-10				
ZTH-2	RDX	20-45	17	48.5	32	2.5
ZTA	HMX	20-45	1 /	46.3	32	2.3
ZTC	CL-20	20-45				

Table 1. Formulations of the tested mixed ester nitramine propellants

3 Test Methods

The surface morphology of the ZTH-1 and ZTH-2 propellants was analyzed using a Field Emission Scanning Electron Microscope (SEM), (Carl Zeiss Instruments, Germany).

The combustion performance was tested using a WJ1753-87 Closed Burst Tester (Chengdu Keda Shengying Technology Co., Ltd., China). The closed burst tester had a volume of 100 mL, with an experimental environmental temperature of 20 °C. A DYY-1 piezoelectric sensor was used. The ignition charge was 1 g of Class C nitrocellulose, with an ignition pressure of 9.8 MPa and a loading density of 0.2 g/cm³.

The impact strength was tested using a ZWJ-0351 simple beam impact testing machine (Yangzhou Daocun Test Machinery Factory, China). The testing conditions were as follows: pendulum mass 5 kg, and square corner of 150 $^\circ$.

The low-temperature drop-weight impact strength was tested using a LDW-100T type low-temperature drop hammer testing machine (China North Industries Group Corporation, 204 Research Institute). Under set conditions, the drop hammer was released without initial velocity to fall freely and strike the fixed end face of the propellant grain. The damage caused was recorded. The testing conditions were as follows: drop hammer mass 5 kg, at temperature –40 °C.

4 Results and Discussion

4.1 SEM results

SEM images of the tested mixed nitrate nitramine propellants containing different RDX particle sizes are shown in Figure 1.

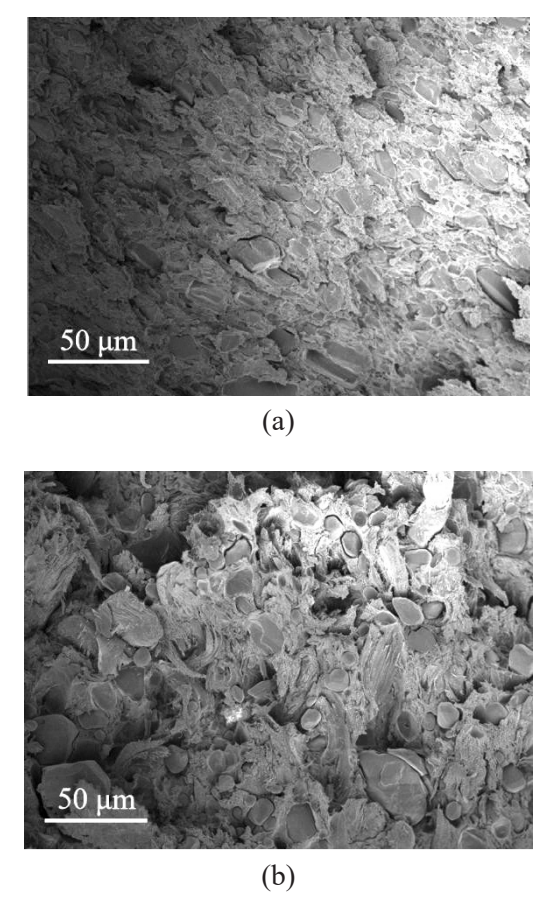


Figure 1. The SEM images of ZTH-1 (a) and ZTH-2 (b) propellants

As shown in Figure 1(a), the ZTH-1 propellant contained the ultrafine RDX particles that were evenly embedded in the nitrocellulose matrix and tightly encapsulated by the nitrocellulose, demonstrating good interfacial bonding strength and structural integrity. This tight integration contributes to improved mechanical properties and energy release efficiency of the propellant. In the ZTH-2 propellant, shown in Figure 1(b), although the RDX particles are more

evenly distributed, their larger particle size leads to the presence of noticeable cavities within the propellant. Additionally, the interfacial bonding strength between the RDX particles and the nitrocellulose matrix is weaker, making the interface prone to delamination at the cut surface. Some RDX particles are even detached from the nitrocellulose matrix. The primary reason for this phenomenon is that as the particle size of RDX is increased, its specific surface area decreases, reducing the contact area with the nitrocellulose matrix and consequently weakening the interfacial bonding force. Moreover, larger RDX particles are more susceptible to stress concentration effects during processing, further weakening the bonding strength with the matrix [14].

4.2 Combustion performance

4.2.1 RDX-based propellants

Figure 2 shows the *P-t* curves of the ZTH-1 and ZTH-2 propellants. As shown in Figure 2, the *P-t* curves of ZTH-1 and ZTH-2 propellants are smooth, with no abnormal fluctuations. The pressure at the beginning of combustion is nearly the same for both, but as combustion progresses, the rate of pressure increase shows a difference. However, the maximum pressure achieved is nearly identical. The pressure increase rate of ZTH-2 is faster, and reaches the maximum pressure approximately 0.9 ms earlier than ZTH-1, indicating that ZTH-2 has a shorter combustion time and faster burn rate. This phenomenon is closely related to the particle size of the RDX. The larger RDX particles used in ZTH-2 result in a smaller specific surface area, which increases the reactivity of the combustion reaction and accelerates the burn rate. Furthermore, the increase in RDX particle size may also alter the thermal conductivity and combustion surface structure of the propellant, further promoting acceleration of the burn rate [16].

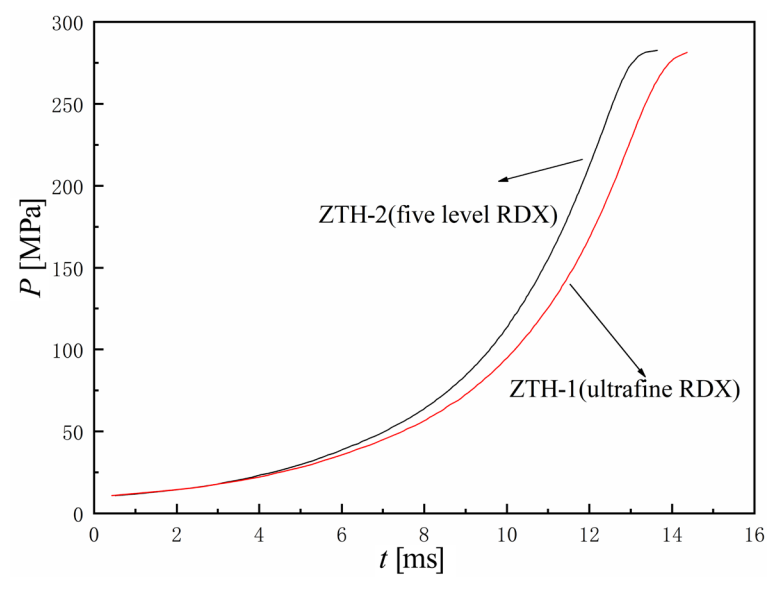


Figure 2. P-t curves of nitramine propellants with different RDX particle sizes

From the burning rate-pressure (*U-P*) curves of nitramine propellants with different RDX particle sizes shown in Figure 3, it can be seen that, within the low-pressure range (10-75 MPa), the burn rate growth rates of ZTH-1 and ZTH-2 are nearly identical, with the curves overlapping. In the medium-pressure range (75-174 MPa), the burn rate of ZTH-2 is significantly higher than that of ZTH-1. When the pressure exceeds 174 MPa, the burn rates of both propellants tend to stabilize, reaching 170 mm·s⁻¹. This phenomenon is closely related to the RDX particle size and combustion mechanism. Firstly, the larger RDX particles used in ZTH-2 result in slower heat absorption and thermal decomposition rate at low pressure. However, as the pressure increases, the thermal decomposition reaction becomes more intense, and the exothermic release significantly increases, which may lead to local detonation of the RDX. This detonation not only rapidly increases the gas-phase temperature but also causes the combustion surface to become uneven, increasing the combustion area and accelerating the reaction rate, thus significantly enhancing the burn rate. By contrast, the ultrafine RDX used in ZTH-1 has a larger specific surface area, requiring more heat for melting at the beginning of combustion [17]. As the pressure increases, the change in its combustion surface is relatively smooth, especially in the high-pressure range, where the rate of change in the specific surface area is small, leading to a relatively lower burn rate. Additionally, the V-class RDX particles in ZTH-2 are less tightly bonded with the nitrocellulose matrix, creating more internal porosity. Some RDX particles may detach from the matrix during combustion and enter the gas phase, further increasing the effective combustion area. The heat released by the RDX combustion in the gas phase then feeds back onto the surface of the propellant, accelerating the combustion reaction. On the other hand, in ZTH-1, the ultrafine RDX is tightly encapsulated by the nitrocellulose, making the structure denser and resulting in smaller changes in the combustion area during combustion. Therefore, the burn rate of ZTH-1 is lower than that of ZTH-2.

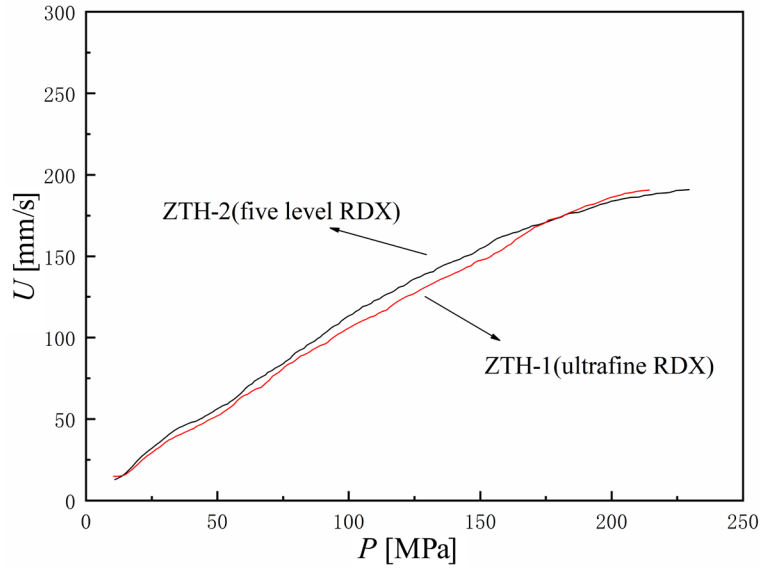


Figure 3. *U-P* curves of nitramine propellants with different RDX particle sizes

Figure 4 shows the gas generation intensity versus combustion mass fraction (Γ - Ψ) curves of propellant samples with different RDX particle sizes. From Figure 4, it can be observed that ZTH-2 propellant exhibits a higher gas generation intensity, with a fuller combustion curve, indicating that ZTH-2 releases energy more intensely and continuously during combustion. This is because the V-class RDX used in ZTH-2 has a larger particle size and a smaller specific surface area. At low pressure, the thermal decomposition rate is slower, and the energy release in the early stage of combustion is relatively gradual. As the pressure increases, the thermal decomposition reaction of the V-class RDX becomes more intense, with a significant increase in exothermic release, leading to a faster gas generation rate and more concentrated energy release in the middle and later stages of combustion. By contrast, the ultrafine RDX used in ZTH-1 has a smaller particle size and a larger specific surface area. The change in

specific surface area during combustion is smaller, resulting in a more uniform combustion reaction. However, the gas generation rate decays more quickly in the later stages of combustion, causing the combustion curve of ZTH-1 to be less full compared to ZTH-2.

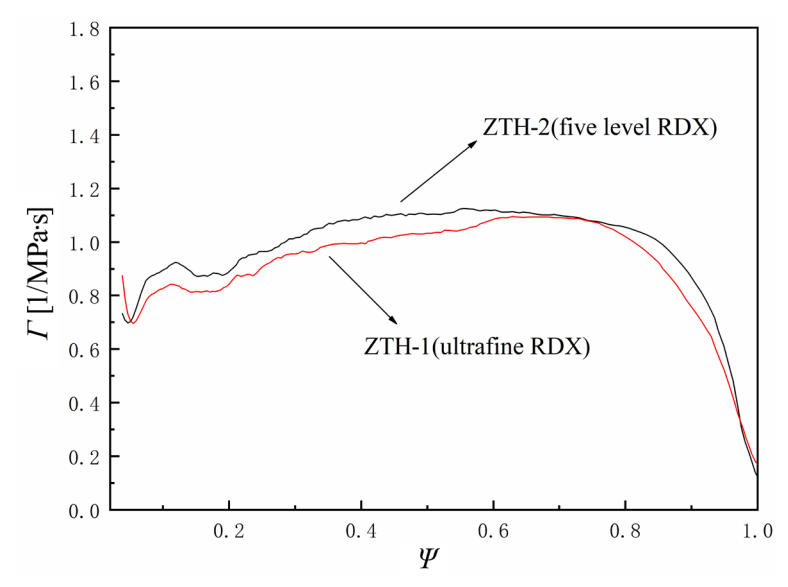


Figure 4. Γ - Ψ curves of nitramine propellants with different RDX particle sizes

4.2.2 Nitramine-based propellants

The burn rate of the propellant mainly depends on the heat released by the condensed-phase reactions of the propellant and the heat feedback from the gasphase reactions, both of which are related to the components of the propellant. To investigate the impact of different types of nitramine explosives on the combustion performance of the propellants, the formulation of the mixed ester nitramine propellants was designed with identical components and contents, except for the type of nitramine explosive. Therefore, samples containing RDX, HMX, and CL-20 as oxidizers were used for the study, and the pressure-time (*P-t*) and burning rate-pressure (*U-P*) curves from the closed burst tester experiments were compared and analyzed, as shown in Figures 5 and 6.

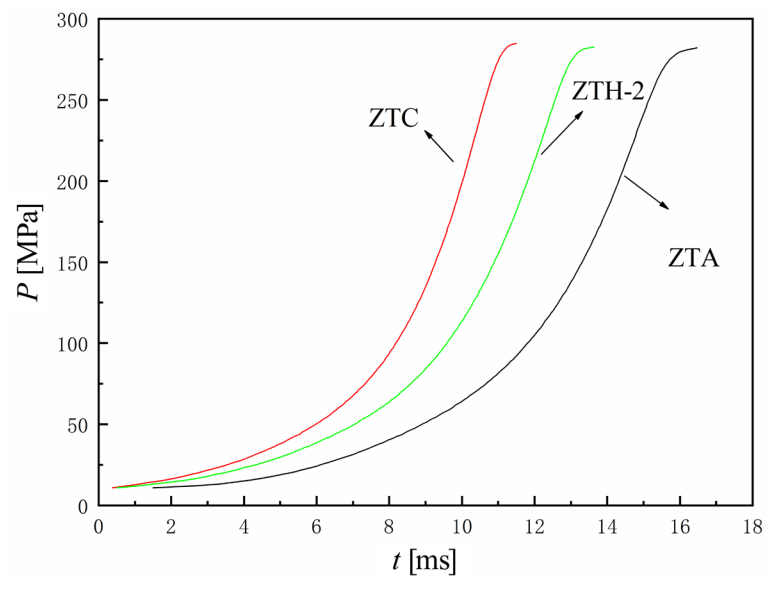


Figure 5. P-t curves for different types of nitramine propellants

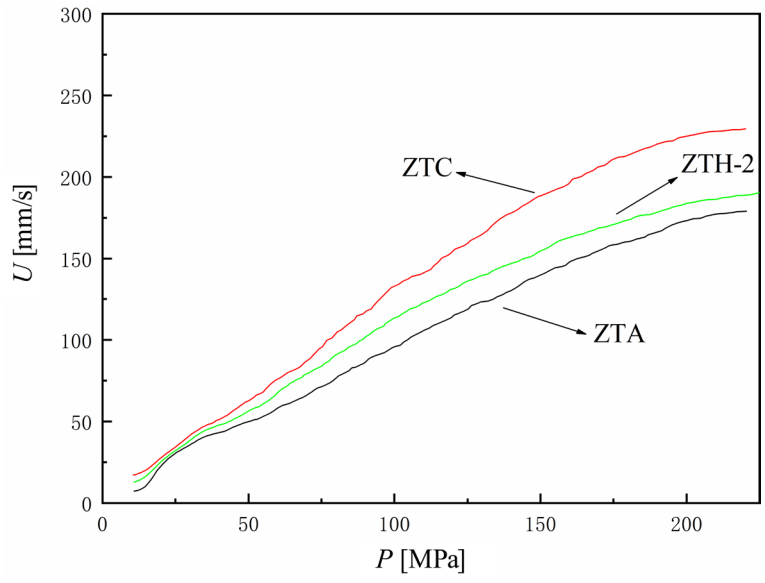


Figure 6. *U-P* curves for different types of nitramine propellants

Figure 5 presents the *P-t* curves of the three nitramine propellants containing CL-20 (ZTC), RDX (ZTH-2), and HMX (ZTA) in a closed vessel, demonstrating

the significant influence of oxidizer type on combustion kinetics. The ZTC propellant exhibits the fastest pressure rise, reaching its peak pressure (285.90 MPa) within 10 ms. This rapid increase is attributed to CL-20's high energy density and low activation energy for thermal decomposition, which accelerate gas-phase reactions and promote intense heat release, driving the pressure surge. By contrast, ZTA propellant shows the slowest pressure rise, requiring 16 ms to attain its peak pressure (282.74 MPa). This delayed response aligns with HMX's high thermal stability and sluggish gas-phase oxidation kinetics. The ZTH-2 propellant displays intermediate behaviour with a 13 ms response time, consistent with RDX's moderate energy density and decomposition rate.

From Figure 6, it can be seen that under the condition of equal nitramine explosive content but different types, the ZTC propellant exhibits the fastest pressure rise rate, reaching the maximum pressure in the shortest time. By contrast, the ZTA propellant containing HMX has the slowest pressure rise rate, reaching the maximum pressure in the longest time. This is because CL-20, as a high-energy density material, contains high strain energy and nitrogen content in its molecular structure, allowing it to quickly release large amounts of gaseous products and heat during combustion, significantly accelerating the pressure rise rate. On the other hand, HMX has a lower energy density, and its thermal decomposition rate and gas generation rate are relatively slower, leading to a more gradual pressure rise. Additionally, the high reactivity of CL-20 allows it to form more reactive intermediate products during combustion, further accelerating the combustion process, whereas the molecular structure of HMX is relatively stable, and its decomposition process requires higher activation energy, resulting in a slower pressure rise rate under the same conditions.

Figure 6 and Table 2 show the U-P curves of propellant samples with the three different types of nitramine explosives and the corresponding burn rates at selected pressure points in the 25-220 MPa pressure range. From Figure 6 and Table 2, it can be observed that within the 25-220 MPa pressure range, the burning rates (U) at the same pressure point follow the order: U(ZTC) > U(ZTH-2) > U(ZTA). The reasons for this are as follows. CL-20 as the primary oxidizer in ZTC(CL-20) propellant, contains the highest nitrogen content in its molecular structure. During thermal decomposition, it releases a significant amount of NO_2 gas. NO_2 not only acts as an oxidizer in the combustion process but also catalyzes condensed-phase reactions, promoting secondary decomposition exothermic reactions. This increases the combustion surface temperature and accelerates the reaction rate, thus leading to the highest burn rate for ZTC(CL-20) propellant during combustion [7]. The thermal decomposition temperature (205 °C) of RDX used in ZTH-2 propellant is significantly lower than that of HMX (278 °C).

In the temperature range of 205 to 278 °C, RDX can reach rapid decomposition conditions earlier and release more NO₂ gas, thus accelerating the combustion reaction rate [18]. The HMX used in the ZTA propellant has a higher melting point and larger decomposition activation energy, resulting in a slower thermal decomposition rate under the same conditions. It releases less NO₂ gas, leading to a lower combustion reaction rate and, therefore, a lower burn rate compared to the ZTC and ZTH-2 propellants. The combustion rate pressure relationship curve is fitted using a segmented exponential model, which is based on the electrostatic Vieille's law [9].

The U-P curves in Figure 6 were fitted using a segmented exponential model $(y = a \cdot x^b)$ with the least squares method. The burn rate pressure exponent (n) and burn rate coefficient (U_1) for the four pressure segments, as well as the burn rate pressure equation over the entire pressure range (50-220 MPa), were obtained. The results are shown in Table 3.

Tresums of the summing face tests of tested miramine propertients									
Propellant	U [mm·s ⁻¹] at pressure [MPa]								
	25	50	75	100	125	150	175	200	220
ZTC	34.9	62.7	95.8	132.3	159.3	189.1	210.4	224.8	229.4
ZTH-1	29.6	52.6	80.8	106.4	126.8	147.1	170.1	183.7	190.5

113.1

95.9

ZTH-2

ZTA

32.1

30.9

56.8

49.9

84.1

71.5

136.2

154.4

119.0 | 139.4 | 158.8 |

170.2

183.6

173.1

188.8

 Table 2.
 Results of the burning rate tests of tested nitramine propellants

Table 3.	Regression data of different types of nitramine propellants at different
	pressure intervals (P_m is the maximum pressure)

Propel- lant	Para- meter		Pressure	P_m	$U = U_1 P^n$, in			
		10-75	75-150	150-220	50-220	$\left \begin{array}{c} I_m \\ [MPa] \end{array} \right $	the range of 50-220 MPa	
ZTC	U_{I}	1.8318	1.6175	13.1102	1.7912	285.90	$1.7912P^{0.9223}$	
	n	0.9080	0.9516	0.5352	0.9223	283.90		
ZTH-1	U_I	1.4504	2.0710	3.5181	1.6418	280 15	$1.6418P^{0.8980}$	
	n	0.9241	0.8524	0.74878	0.8980	200.13		
ZTH-2	U_I	1.3805	2.0716	11.9524	2.2675	202.00	$2.2675P^{0.8387}$	
	n	0.9561	0.8650	0.5145	0.8387	202.90		
ZTA	U_{I}	0.7861	1.1419	5.0173	1.3873	282.74	$1.3873P^{0.9160}$	
	n	1.0679	0.9613	0.6666	0.9160	202.74	1.30/31	

From Table 3, it can be seen that, as the pressure increases, the pressure exponent for the propellants with different types of nitramine explosives tends to

decrease, following the order: $n_{(10-75 \text{ MPa})} > n_{(75-150 \text{ MPa})} > n_{(150-220 \text{ MPa})}$. This indicates that when the particle size was the same, although the ZTH-2 propellant containing RDX has a higher pressure exponent than the ZTC propellant containing CL-20 at low pressures, it has the lowest pressure exponent in the medium, high, and entire pressure ranges. By contrast, the ZTC propellant containing CL-20 has the highest pressure exponent in the entire pressure ranges (50-220 MPa). This is because RDX has a lower melting point and energy density, and its thermal decomposition process is relatively slow, leading to a slower energy release rate. As a result, at the same pressure, the burn rate is relatively lower. On the other hand, CL-20 has a higher energy density and lower thermal decomposition activation energy, allowing it to quickly release a large amount of energy during combustion, significantly increasing the burn rate [19].

4.3 Impact strength

ZTH-2

The impact strength (a_{κ}) is an indicator of the toughness of a propellant with a specific geometry under certain test conditions [20]. It represents the object's resistance to sudden impact. Typically, it is expressed as the work consumed to break a specified propellant sample under constant temperature and load. When a propellant cannot withstand sudden mechanical forces and fractures, it is of the propellants containing different nitramine explosives at -40 °C.

referred to as the propellant's brittleness. The impact resistance characteristics of the propellants were measured using a pendulum impact testing machine, which determines the energy consumed during the fracture process of the propellant under high-speed pendulum impact. Table 4 shows the impact resistance strength

Impact strength (α_{κ}) The standard deviation [%] Sample $[kJ \cdot m^{-2}]$ ZTA 8.61 0.90 **ZTC** 7.90 0.70 ZTH-1 8.40 1.12

1.19

8.70

Impact strength (α_{κ}) of nitramine propellants using a simple beam Table 4. test at -40 °C

From Table 4, it can be seen that when the content and particle size of the nitramine explosives are the same, the impact strength of the different nitramine propellants follows the order: $\alpha_{\kappa}(ZTH-2) > \alpha_{\kappa}(ZTA) > \alpha_{\kappa}(ZTH-1) > \alpha_{\kappa}(ZTC)$. Among these, the impact strength of ZTH-2 propellant is the highest, being 10.13% higher than that of the ZTC propellant. This phenomenon is closely related to the molecular structure of the nitramine crystals, their mechanical properties, and their interaction with the binder interface [21].

CL-20 molecules have a larger relative molecular mass than HMX and RDX. For nitramine explosive particles of the same size, the internal molecular spatial configuration of CL-20 crystals is larger. When subjected to external impact forces, cracks are more likely to propagate along weak crystal planes, weakening the support provided by the particles to the cross-section and creating stress concentration points, thereby reducing impact resistance [22]. The nitro group (-NO₂) in the nitramine and the hydroxyl group (-OH) in the polymer chains of the binder are more likely to form hydrogen bonds, which increases rigidity and weakens the flexibility of the binder's polymer chains at the interface. This further reduces the impact resistance strength. The crystal structures of RDX (ZTH-2) and HMX (ZTA) are more symmetrical, with fewer internal defects. Under low-temperature conditions, they can better maintain structural integrity, exhibiting excellent impact resistance performance. By contrast, the high strain energy in the CL-20 crystal structure provides superior energy characteristics but also makes it more prone to brittle failure under low-temperature conditions, thus reducing its impact resistance strength [23]. According to the hot spot theory, when the explosive is subjected to mechanical external forces such as impact and friction, the pores of the explosive particles are adiabatic and compressed to form local hot spots, and in the process of impact (friction), the more hot spots that are formed inside it, the more likely it is to deflagrate [24]. ZTH-2 may have fewer defects on the surface, so it has a higher impact strength.

4.4 Low temperature drop-weight impact strength test

Low-temperature drop-weight impact strength is determined by releasing a known mass drop hammer through a braking device under set conditions, allowing it to fall free and strike the fixed end face of the propellant sample. Table 5 shows the results of the drop-weight impact strength tests performed at $-40\,^{\circ}\mathrm{C}$ for the nitramine propellants.

 Table 5.
 Table of low-temperature drop-weight impact strength test data for the different nitramine propellants

Sample	Hammer weight [kg]	Fall height [cm]	Broken rate [%]
ZTC			100
ZTH-1		80	70
ZTH-2] 3	80	50
ZTA			20

From Table 5, it can be observed that the three types of nitramine propellants exhibit significant differences in their low-temperature impact strengths (drop weight test), with the strength order being: [ZTA] > [ZTH-2] > [ZTH-1] > [ZTC]. Among these, the low-temperature mechanical performance (drop weight test) of ZTA samples is slightly better than that of ZTH propellants, while the low-temperature mechanical performance of ZTC propellant is the poorest. This is due to the following reasons:

- Elastic modulus: The order of the elastic modulus for the three types of nitramine crystals is [CL-20] > [RDX] > [HMX]. A smaller elastic modulus indicates that the material is more likely to undergo elastic deformation under external forces, which allows it to better absorb the impact energy applied to it, resulting in better mechanical performance.
- Friction coefficient: The friction coefficient is also an important factor affecting low-temperature mechanical performance. The order of friction coefficients for the three nitramine explosives is [CL-20] < [RDX] < [HMX]. When the propellant matrix is subjected to axial forces, HMX, with a higher friction coefficient, indicates that its crystal surface is rougher. This roughness leads to more energy absorption when sliding under external forces, which contributes to better mechanical performance.

5 Conclusions

This study has investigated the coupling effect mechanism between the particle size of RDX and the CL-20/HMX explosive type on the high-pressure combustion behaviour and extreme-environment mechanical properties of mixed ester nitramine propellants, offering vital theoretical support for the development of high energy insensitive propellants.

- Compared with the ZTH-1, the larger-particle-size RDX (20-45 μm) in ZTH-2 enhances the combustion rate by 12.3% and intensifies gas generation concentration by 37% at 174 MPa, primarily through increased propellant porosity and amplified thermal feedback effects, thereby establishing a novel control path for high-combustion-rate applications.
- ♦ Of the different types of mixed ester nitramine propellants containing RDX, HMX, and CL-20, the burn rate follows the order: *U*(ZTC) > *U*(ZTH-2) > *U*(ZTH-1)> *U*(ZTA). The pressure index of ZTH-2 propellant containing RDX is the smallest, while the ZTC propellant containing CL-20 has the largest pressure index.
- ♦ There are significant differences in the low-temperature impact strength

- between the three different types of nitramine propellants. The simple beam test indicates that the impact strength of the propellant samples follows the order: $\alpha_{\kappa}(ZTH-2) > \alpha_{\kappa}(ZTA) > \alpha_{\kappa}(ZTH-1) > \alpha_{\kappa}(ZTC)$. In the low-temperature drop-weight impact strength test, the impact strength order is: [ZTA] > [ZTH-2] > [ZTH-1]> [ZTC].
- ♦ Although ZTH-1 and ZTH-2 have exactly the same formulation, their performance shows significant differences due to the critical differences in RDX particle size. The similar chemical composition ensures comparable theoretical energy output and maximum pressure in a confined detonation. ZTH-2 shows a significantly higher combustion rate and gas generation intensity, attributed to its increased porosity and enhanced thermal feedback effect; whereas the more densely structured ZTH-1 exhibits a lower combustion rate. In terms of mechanical properties, the better interface binding of ZTH-1 did not translate into the highest impact strength; ZTH-2 has a higher impact strength value (8.70 kJ·m⁻²).
- This study reveals an inherent compromise between high-energy explosives and mechanical properties.

References

- [1] Liu, J.; Liu, Z.; Yang, J.; Xu, B.; Chen, F. The Influence of Nano-Composite Metal Oxides on the Thermal Decomposition Performance of RDX. *J. Phys.: Conf. Ser.* **2024**, *2819*(1): 012008-012008; https://doi.org/10.1088/1742-6596/2819/1/012008.
- [2] Chen, J.; Meng. D.Q.; Zhang, P.A.; Deng, J.R. Interactions between a Neutral Polymeric Bonding Agent and Nitramine Explosives and Their Influencing Factors. *Energ. Mater. Front.* **2024**, *5*(3): 248-256; https://doi.org/10.1016/j.enmf.2024.03.002.
- [3] Xie, W.X.; Wei, H.J.; Zhang, W. Energetic Characteristics of BAMO/THF Low Signature Propellant Containing CL-20 as Oxidizer. (in Chinese) *J. Sichuan Ordnance* **2012**, *33*(9): 109-112.
- [4] Wang, M.; Li, X.; Li, S.; Li, W.; Stewart, C.; Yang, Y.; Liu, F. Reinforcing Effect of Trifluoromethyl/Amino-modified Neutral Polymeric Bonding Agents on Interfacial Bonding of Fluoropolymer/Nitramine Energetic Composites-based High-Energy Polymer Bonded Explosives. *Iran. Polym. J.* **2023**, *32*(6): 729-737; https://doi.org/10.1007/s13726-023-01162-z.
- [5] Elghafour, A.M.A.; Radwan, M.A.; Mostafa, H.E.; Fahd, A.; Elbasuney, S. Highly Energetic Nitramines: A Novel Platonizing Agent for Double-base Propellants with Superior Combustion Characteristics. *Fuel* 2018, 227: 478-484; https://doi. org/10.1016/j.fuel.2018.04.117.
- [6] Lavoie, J.; Petre, C.F.; Durand, S.; Dubois, C. Stability and Performance of Gun

- Propellants Incorporating 3,6-Dihydrazino-s-tetrazine and 5-Aminotetrazolium Nitrate. *J. Hazard. Mater.* **2019**, *363*: 457-463; https://doi.org/10.1016/j.jhazmat.2018.09.088.
- [7] Wu, Y.G.; Wu, X.Q.; Chen, H.W.; Zhang, L.; Zhang, C. Performance of Nitramine Propellants with Different Phases of HMX. (in Chinese) *Chin. J. Energ. Mater.* **2009**, *17*(2): 206-209.
- [8] Zhang, F.; Zhu, D.P.; Liu, Q.; Liu, Z.T.; Du, P. Study on the Effect of RDX Content on the Properties of Nitramine Propellant. *Def. Technol.* **2017**, *13*(4): 246-248; https://doi.org/10.1016/j.dt.2017.05.020.
- [9] Sinditskii, V.P.; Chernyi, A.N.; Egorshev, V.Y.; Dashko, D.V.; Goncharov, T.K.; Shishov, N.I. Combustion of CL-20 Cocrystals. *Combust. Flame* 2019, 207: 51-62; https://doi.org/10.1016/j.combustflame.2019.05.039.
- [10] Wei, L.; Wang, Q.L.; Liu, S.W.; Zhu, C.Y.; Guo, F.; Zhang, Y.B. Application of High Energy Density Compounds CL-20, DNTF, and AND in High Energy Propellant. *Chin. J. Explos. Propellants.* 2009, 32(2): 17-20; https://doi.org/10.14077j. issn.1007-7812.2007.01.011.
- [11] Wang, S.; Yang, L.; Han, J.; Yan, Z. MOF as the Rigid Shell to Improve the Mechanical Sensitivity of Nitramine Explosives. *Mater. Lett.* **2022**, *306* paper 130940; https://doi.org/10.1016/j.matlet.2021.130940.
- [12] Tian, Y.; Wang, Y.B.; He, W.D.; Dong, J. Effects of TMETN Content and NC Nitrogen Content on the Mechanical Properties of TMETN/NG Mixed Nitrate Propellants. (in Chinese) *Chin. J. Explos. Propellants* 2019, 42(2): 175-179; https://doi.org/10.14077/j.issn.1007-7812.2019.02.012.
- [13] Liu, J.; Zhang, L.H.; Ma, Z.L.; Xiao, Z.L. Study on Mechanical Properties of Multi-Phase Gun-Propellant Containing RDX. (in Chinese) *Chem. Propellants Polym. Mater.* **2013**, *11*(4): 87-89; https://doi.org/10.16572/j.issn1672-2191.2013.04.032
- [14] Xu, G.Z.; Gao, X.D.; Jin, G.L.; Wang, D.Q.; Zhang, Z.M.; Tan, T.Y.; Qin, Y.; Liu, J.; Li, F.S. Preparation of Nano-RDX-Based Polymer-Bonded Explosive and Its Improved Mechanical and Detonation Properties. *Combust. Explos. Shock Waves*, **2023**, *59*(1): 103-109; https://doi.org/10.15372/fgv20230112.
- [15] Jia, X.; Wang, J.; Huo, C.; Tan, Y.; Zhang, Y. Effective Insensitiveness of Melamine Urea-Formaldehyde Resin via Interfacial Polymerization on Nitramine Explosives. *Nanoscale Res. Lett.* 2018, 13 paper 402; https://doi.org/10.1186/s11671-018-2803-z.
- [16] Han, J.C. *Preparation and Properties of Modified Single-based Gun Propellant.* Master's Thesis, North University of China, **2019**.
- [17] Bing, C.; Zhang, L.H. The Influence of Particle-size of RDX on the Impact Resistance of DAGR Nitramine Gun Propellant. (in Chinese) *Fine Chemical Intermediates* **2017**, *47*(04): 51-58; https://doi.org/10.19342/j.cnki.issn.1009-9212.2017.04.012.
- [18] Fu, Y.; Wang, B.B.; Xu, B.; Liao, X. Effect of RDX on Combustion Performance of Modified Single Base Propellant. (in Chinese) *Chin. J. Energ. Mater.* 2017, 25(2): 161-166; https://doi.org/10.11943/j.issn.1006-9941.2017.02.012.

- [19] Ren, X.X.; Zhu, Y.J.; Zhao, S.X.; Han, Z.; Yao, L. The Relationship between Micromechanical Property and Friction Property of Four Kinds of Energetic Crystals. (in Chinese) *Mater. Rep.* **2019**, *33*(1): 448-452.
- [20] Liu, J.H.; Zhao, H.L.; He, C.H.; Jin, J.W.; Zhao, B.M.; Wang, Q.L.; Zhang, Z.Z. Method to Determine the Impact Strength of Triple-base Gun Propellant Based on Strain Energy Density. *Propellants Explos. Pyrotech.* 2020, 45(9): 1407-1415; https://doi.org/10.1002/prep.202000012.
- [21] Pei, B.L.; Peng, S.; Cao, R.; Zhao, C.Y. Dynamics of CL-20/HMX Co-Crystal in Nitrate Plasticized GAP Adhesive. *J. Solid Rocket Technol.* **2020**, *43*(5): 581-586; https://doi.org/10.7673/j.issn.1006-2793.2020.05.006.
- [22] Zhang, C.; Zhang, X.; Dai, J.; Sun, Y. Towards Revealing the Catalytic Mechanism of Copper Oxide on the Decomposition of RDX in Modified Double-Base Propellants. *Fuel* **2025**, *384* paper 133952; https://doi.org/10.1016/j.fuel.2024.133952.
- [23] Bray, K.N.C.; Champion, M.; Libby, P.A. Theoretical Study of the Turbulent Combustion of Nitramine Propellant. *Combust. Sci. Technol.* 2017, 189(7): 1216-1240; https://doi.org/10.1080/00102202.2017.1280481.
- [24] Zhou, S.P.; Wu, F.; Tang, G.; Wang, Y.; Pang, A.M. Effects of 2CL-20/HMX Cocrystals on the Thermal Decomposition Behavior and Combustion Properties of Polyether Solid Propellants. *Energ. Mater. Front.* **2021**, *2*(2): 96-104; https://doi.org/10.1016/j.enmf.2021.03.003.

Authorship contribution statement

Jun Dong: conception, foundations, performing the experimental part

Jinyu Peng: methods

Chunzhi Li: performing the experimental part

Jiangyang Ou: methods Jinrui Liu: methods

Submitted: March 30, 2025 Revised: September 29, 2025

First published online: September 30, 2025